ANALYSIS OF A FINITE DIFFERENCE SCHEME WITH ADAPTIVE SPATIAL OPERATOR FOR THE ACOUSTIC WAVE EQUATION

A. W. Camargo and L. T. Santos

email: *alexandrewac.fox@gmail.com, lucio@ime.unicamp.br*

keywords: *Finite Differences, Wave Equation, Adaptive Operators*

ABSTRACT

Most of Finite Difference (FD) methods used in seismic modeling are based on fixed length spatial operators. These operators are chosen observing computacional cost, stability and dispersion criteria. In this work we analyse a FD scheme with an adaptive spatial operator which reduces the computational cost but not the accuracy. The idea is to use long operators in low velocity regions and short operators in high velocity ones. The analysis is made in the one- and two-dimensional cases, but the results can be extended for 3D models.

INTRODUCTION

Seismic modeling simulates the wave propagation in subsurface. One of the fundamental basis of seismic modeling is the acoustic wave equation which requires, with rare exceptions, efficient numerical methods to be solved. Due to their simple implementation, algorithms based on Finite Differences (FD) are preferred to solve the acoustic wave equation (Liu and Sen, 2009, 2011; Dablain, 1986; Kelly et al., 1976). In addition, if a FD method satisfies all the criteria of stability and dispersion, the numerical solution is of excelent quality.

If we are not concerned with computacional costs, we can use a spatial grid based on the the minimum velocity. As the source usually is fixed in the modeling, its main frequency is also fixed and then the wavelength in the region with low velocity is smaller than in the region with high velocity. Therefore, the accuracy is greater in the high velocity regions. There are many variants of FD method to increase efficiency without decreasing accuracy, or to increase accuracy without decreasing efficiency or to increase both efficiency and accuracy. See, e.g., Virieux (1984), Virieux (1986), Finkelstein and Kastner (2007) and Bartolo et al. (2012).

For fixed spatial and time steps, when we use the same length for the spatial operator of the FD scheme, we reach greater accuracy in higher velocity regions than in lower ones. Therefore, it would be more efficient if we could choose the length of the spatial operator according to the velocity. In this work we analyse one approach introduced by Liu and Sen (2011), based on a FD scheme with an adaptive spatial operator. The length of the spatial operator is chosen based on the analysis of the stability and dispersion in each velocity region, in such a way that the length decreases with increasing velocity. Numerical examples illustrate the approach.

Let $\mathbf{x} \in I\!R^n$ $(n = 1, 2, 3)$ be the space variable, $t \in I\!R^n$ be the temporal variable and $c(\mathbf{x})$ be the wave propagation velocity in the acoustic model. The acoustic wave equation is given by

$$\frac{1}{c(\mathbf{x})^2} U_{tt}(\mathbf{x}, t) - \Delta U(\mathbf{x}, t) = F(\mathbf{x}, t), \tag{1}$$

where $U(\mathbf{x}, t)$ is the scalar wavefield, Δ denotes the Laplacian operator, and $F(\mathbf{x}, t)$ is the source term. For $n = 1$ we will consider $\mathbf{x} = x$ and for $n = 2$, $\mathbf{x} = (x, z)$.

ONE-DIMENSIONAL MODELING

We first analyse the one-dimensional case ($n = 1$) and describe the FD scheme and the method that will be used to choose the length of the space operator, according to the velocity. Applying a second-order FD operator in time and a $(2M)$th-order FD operator in space, we get

$$U_{tt}(x_j, t_k) \approx \frac{1}{\Delta t^2}\left[-2u_j^k + (u_j^{k-1} + u_j^{k+1})\right], \tag{2}$$

$$\Delta U(x_j, t_k) = U_{xx}(x_j, t_k) \approx \frac{1}{\Delta x^2}\left[a_{0,j}u_j^k + \sum_{m=1}^{M} a_{m,j}(u_{j-m}^k + u_{j+m}^k)\right], \tag{3}$$

where $u_j^k = U(x_j, t_k)$, $x_j = x_0 + j\Delta x$, $t_k = k\Delta t$, with $j = 0, 1, \ldots, J$ and $k = 0, \ldots, K$. The coefficients $a_{m,j}$ are given by (Liu and Sen, 2009; Finkelstein and Kastner, 2007)

$$a_{m,j} = \frac{(-1)^{m+1}}{m^2} \prod_{n=1, n\neq m}^{M} \left|\frac{n^2 - r_j^2}{n^2 - m^2}\right|, \quad m = 1, 2, \ldots, M, \tag{4}$$

and

$$a_{0,j} = -2\sum_{m=1}^{M} a_{m,j}, \tag{5}$$

where $r_j = c(x_j)\Delta t/\Delta x$ are the Courant numbers. Substituting equations (2) and (3) into equation (1), we obtain the following recursion formula,

$$u_j^{k+1} = 2u_j^k - u_j^{k-1} + r_j^2\left[a_{0,j}u_j^k + \sum_{m=1}^{M} a_{m,j}(u_{j-m}^k + u_{j+m}^k)\right] + [c(x_j)\Delta t]^2 F(x_j, t_k). \tag{6}$$

Stability Analysis

The stability of the method can be obtained by the Von Neumman analysis (Strikwerda, 1989). Taking

$$u_j^k = A^k e^{i(j\xi\Delta x)}, \tag{7}$$

where ξ is the wavenumber and A is the amplification factor. The FD scheme is stable if the amplification factor is such that $|A| \leq 1$. Substituting equation (7) into equation (6), without considering the source term, we have

$$A^2 - \beta_j A + 1 = 0, \tag{8}$$

where

$$\beta_j = 2 + 2r_j^2 \sum_{m=1}^{M} a_{m,j}(\cos(m\xi\Delta x) - 1). \tag{9}$$

Solving the above equation for A, we find

$$A = \frac{\beta_j \pm \sqrt{\beta_j^2 - 4}}{2}. \tag{10}$$

Therefore, if $|\beta_j| \leq 2$ we have $|A| \leq 1$, and then the FD scheme is stable. Assuming that, in general, the error increases with the wavenumber, we can consider the Nyquist wavenumber $\xi_{Nyq} = \pi/\Delta x$ as the maximum value for ξ. Computing β_j for $\xi = \xi_{Nyq}$ we obtain

$$\beta_j = 2 + 2r_j^2 \sum_{m=1}^{M} a_{m,j}(\cos(m\pi) - 1) = 2 - 4r_j^2 \sum_{m=1}^{\overline{M}} a_{2m-1,j}, \tag{11}$$

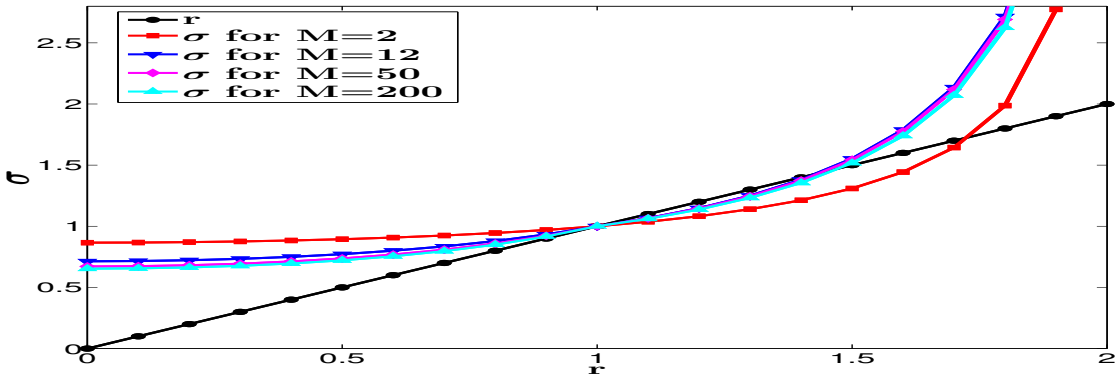

Figure 1: Variation of σ with r for different values of the length operator M, in the one-dimensional case.

where $\overline{M}$ is the integer part of the half of M. Now, since from equation (4), $a_{2m-1,j} > 0$, the method is stable if

$$r_j \leq \Big(\sum_{m=1}^{\overline{M}} a_{2m-1,j} \Big)^{-1/2} \equiv \sigma(r_j). \tag{12}$$

In Figure 1 we show the behaviour of $\sigma(r_j)$ for different values of M. From that figure, we can conclude that relation (12) is satisfied if $r_j \leq 1$.

Dispersion Analysis

The condition $r_j \leq 1$ guarantees the stability of the FD scheme, but not prevent it for numerical errors due to dispersion. The dispersion occurs when the phase velocity v_j and propagation velocity $c_j = c(x_j)$ are different. The difference is measured by the ratio between them, given by

$$\psi_j = \frac{v_j}{c_j} = \frac{\varphi_j/\xi}{c_j}, \tag{13}$$

where ξ is the wavenumber and φ_j is the dispersion angular frequency determined by plane wave theory applied to the recursion formula (6). Taking

$$u_j^k = e^{i(\xi x_j - \varphi_j t_k)}, \tag{14}$$

and substituting it into equation (6), we find

$$\varphi_j = \frac{2}{\Delta t} \arcsin \sqrt{r_j^2 \sum_{m=1}^{M} a_{m,j} \sin^2 \Big(\frac{m\gamma}{2} \Big)}, \tag{15}$$

where $\gamma = \xi \Delta x$. Therefore,

$$\psi_j = \frac{2}{r_j \gamma} \arcsin \sqrt{r_j^2 \sum_{m=1}^{M} a_{m,j} \sin^2 \Big(\frac{m\gamma}{2} \Big)}. \tag{16}$$

If ψ_j is far from 1, the FD scheme is very dispersive. Therefore, we want some condition that makes $\psi_j \approx 1$. Figure 2 depict the dispersion curves, i.e., the variation of ψ_j with γ, in the cases $M = 2$ and $M = 12$ for some values of r_j in the interval $(0, 1)$. We can observe that the region for γ that makes $\psi \approx 1$ increases with the increasing of M.

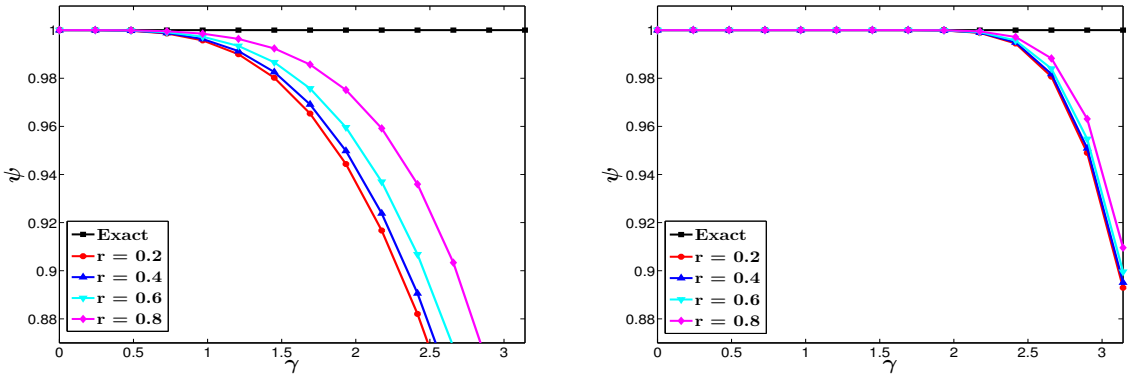

Figure 2: Dispersion variation with γ for different values of r and $M = 2$ (left) and $M = 12$ (right).

The Choice for Δx, Δt and M

Before presenting the method that chooses the length operator M, we will explain why Δx can be fixed without loss of accuracy or stability. Based on Figure 2, given $\epsilon > 0$ and $M \geq M_{min} \geq 1$, there exist γ_{max} and r_{max} such that,

$$|\psi - 1| \leq \epsilon \quad \text{if} \quad \gamma \leq \gamma_{max} \quad \text{and} \quad r \leq r_{max}. \tag{17}$$

Denoting by λ the wavelength and f the frequency, we can write

$$\gamma = \xi \Delta x = \frac{2\pi \Delta x}{\lambda} = \frac{2\pi f \Delta x}{c}. \tag{18}$$

Assuming that the maximum frequency is f_{max} and the minimum velocity is c_{min}, we have that

$$\gamma \leq \gamma_{max} \quad \text{if} \quad \Delta x \leq \frac{\gamma_{max} c_{min}}{2\pi f_{max}}. \tag{19}$$

Once Δx is chosen, Δt can be given by

$$\Delta t \leq \frac{\Delta x \, r_{max}}{c_{max}}, \tag{20}$$

where c_{max} is the maximum velocity. Remember that for the FD scheme to be stable is necessary that $r_{max} < 1$. For example, let us consider the case of $f_{max} = 30$ Hz, $c_{min} = 1.5$ km/s, $c_{max} = 5$ km/s, and the tolerance for the dispersion $\epsilon = 0.05$. For $M_{min} = 2$, from Figure 2 we can choose $\gamma_{max} = 2$ and $r_{max} = 0.5$. Therefore, we can take $\Delta x \approx 15$ m and $\Delta t \approx 1.5$ ms.

Now, let us explain how to choose the length operator M_j according to the velocity c_j. For a fixed M the error in the FD scheme can be measured by the difference between FD and exact propagation times,

$$\mu(M, c_j) = \left| \frac{\Delta x}{v_j} - \frac{\Delta x}{c_j} \right| = \frac{\Delta x}{c_j} \left| \frac{1}{\psi_j} - 1 \right|, \tag{21}$$

where ψ_j is given by equation (16) with

$$\gamma = \frac{2\pi f_{max} \Delta x}{c_j}. \tag{22}$$

Therefore, for a fixed maximum error $\eta > 0$, we choose M_j as the minimum $M \geq M_{min}$ such that

$$\mu(M, c_j) \leq \eta. \tag{23}$$

Following the numerical example above, in Figure 3 we show the values of M_j according to equation (23) for different values of c_j and η.

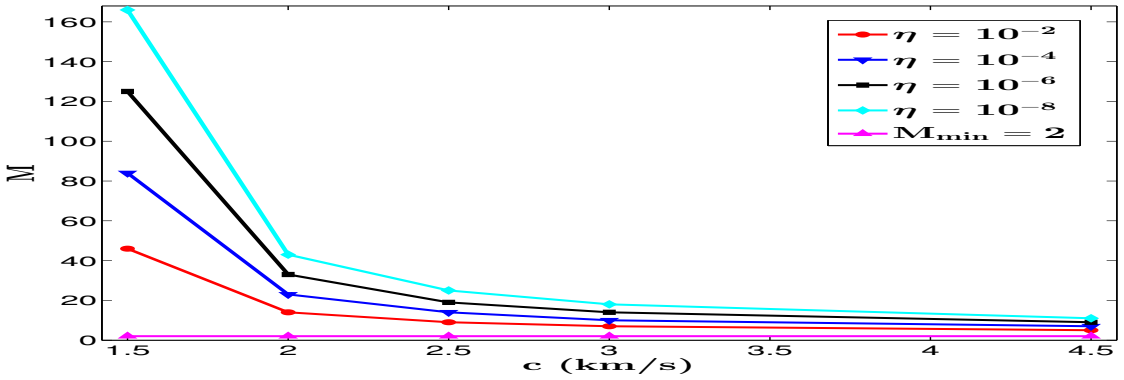

Figure 3: Variation of the length operator M with the velocity c for different values of η.

TWO-DIMENSIONAL MODELING

The analysis of the two-dimensional case is very similar to what we have done in the previous section. For $n = 2$ we consider the following FD scheme,

$$U_{tt}(x_j, z_\ell, t_k) \approx \frac{1}{\Delta t^2}\left[-2u^k_{j,\ell} + (u^{k-1}_{j,\ell} + u^{k+1}_{j,\ell})\right], \tag{24}$$

$$U_{xx}(x_j, z_\ell, t_k) \approx \frac{1}{\Delta x^2}\left[a_{0,j,\ell}u^k_{j,\ell} + \sum_{m=1}^{M} a_{m,j,\ell}(u^k_{j-m,\ell} + u^k_{j+m,\ell})\right], \tag{25}$$

$$U_{zz}(x_j, z_\ell, t_k) \approx \frac{1}{\Delta z^2}\left[a_{0,j,\ell}u^k_{j,\ell} + \sum_{m=1}^{M} a_{m,j,\ell}(u^k_{j,\ell-m} + u^k_{j,\ell+m})\right], \tag{26}$$

where $u^k_{j,\ell} = U(x_j, z_\ell, t_k)$, $x_j = x_0 + j\Delta x$, $z_\ell = z_0 + \ell\Delta z$, $t_k = k\Delta t$, with $j = 0, 1, \ldots, J$, $\ell = 0, 1, \ldots, L$ and $k = 0, \ldots, K$. We will consider a regular grid, i.e, $\Delta x = \Delta z$, and the coefficients $a_{m,j,\ell}$ are given by the solution of the followig Vandermonde linear system (Liu and Sen, 2009; Finkelstein and Kastner, 2007)

$$\sum_{m=1}^{M} m^{2n} a_{m,j,\ell} = \frac{r^{2n-2}_{j,\ell}}{f_n(\theta)}, \quad n = 1, 2, \ldots, M, \tag{27}$$

$$a_{0,j,\ell} = -2\sum_{m=1}^{M} a_{m,j,\ell}, \tag{28}$$

where $r_{j,\ell} = c(x_j, z_\ell)\Delta t/\Delta x$ are the Courant numbers, $f_n(\theta) = \cos^{2n}(\theta) + \sin^{2n}(\theta)$, and θ is the propagation angle. Observe that $a_{m,j,\ell} \equiv a_{m,j,\ell}(\theta)$ and that function f_n is periodic, i.e., $f_n(\theta) = f_n(b\pi/2 \pm \theta)$, with b an integer. Substituting equations (24)–(26) into equation (1) with $n = 2$, we obtain the following recursion formula,

$$u^{k+1}_{j,\ell} = 2u^k_{j,\ell} - u^{k-1}_{j,\ell} + r^2_{j,\ell}\left[2a_{0,j,\ell}u^k_{j,\ell} + \sum_{m=1}^{M} a_{m,j,\ell}(u^k_{j-m,\ell} + u^k_{j+m,\ell} + u^k_{j,\ell-m} + u^k_{j,\ell+m})\right] + F(x_j, z_\ell, t_k). \tag{29}$$

Stability Analysis

Similar to the one-dimensional, we use the Von Neumman Analysis. Taking,

$$u^k_{j,\ell} = A^k e^{i(j\xi_x\Delta x)} e^{i(\ell\xi_z\Delta x)}, \tag{30}$$

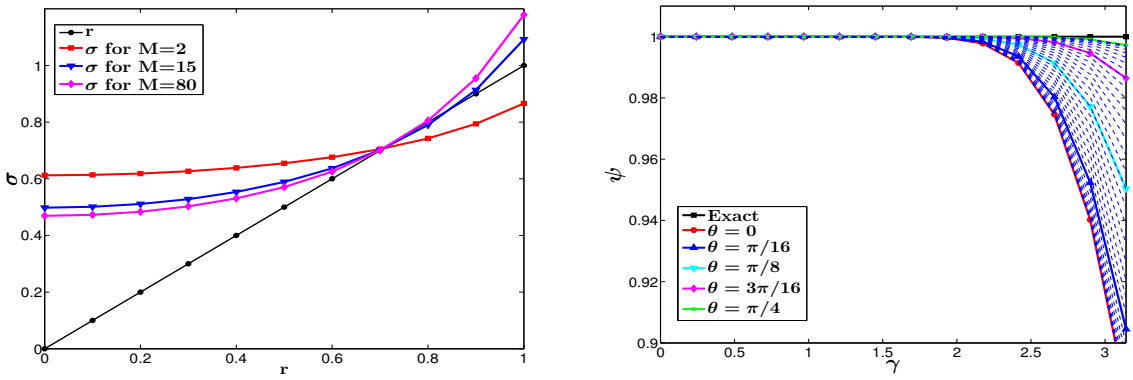

Figure 4: Right: Variation of σ with r for different values of the length operator M, in the two-dimensional case. Left: Dispersion variation with the propagation angle.

where ξ_x and ξ_z are the wavenumbers in x and z,respectively, and A is the amplification factor. Substituting equation (30) into equation (29), we find

$$A^2 - \beta_{j,\ell} A + 1 = 0, \tag{31}$$

where

$$\beta_{j,\ell} = 2 + 2r_{j,\ell}^2 \sum_{m=1}^{M} a_{m,j,\ell}(\cos(m\xi_x \Delta x) + \cos(m\xi_z \Delta x) - 2). \tag{32}$$

Solving the above equation for A, we obtain

$$A = \frac{\beta_{j,\ell} \pm \sqrt{\beta_{j,\ell}^2 - 4}}{2}. \tag{33}$$

Again, if $|\beta_{j,\ell}| \leq 2$, we have $|A| \leq 1$, and then the FD scheme is satble. Using the same argument as in the one-dimesnsional case, i.e., that the error increases with the wavenumber, we can take the Nyquist wavenumber, $\xi_{Nyq} = \pi/\Delta x = \pi/\Delta z$, as the maximum values for ξ_x and ξ_z. Computing $\beta_{j,\ell}$ for $\xi = \xi_{Nyq}$, we find

$$\beta_{j,\ell} = 2 + 4r_{j,\ell}^2 \sum_{m=1}^{M} (\cos(m\pi) - 1) = 2 - 8r_{j,\ell}^2 \sum_{m=1}^{\overline{M}} a_{2m-1,j,\ell}. \tag{34}$$

Since from equation (27), $a_{2m-1,j,\ell} > 0$, the method is stable if

$$r_{j,\ell} < \left(2 \sum_{m=1}^{\overline{M}} a_{2m-1,j}\right)^{-1/2} \equiv \sigma(r_{j,\ell}). \tag{35}$$

In Figure 4 we can observe the behaviour of $\sigma(r_{j,\ell})$ for differente values of M. From that figure, we can conclude that relation (35) is satisfied if $r_{j,\ell} \leq 0.7$.

Dispersion Analysis

Similarly to the one-dimensional case, we define

$$\psi_{j,\ell} = \frac{v_{j,\ell}}{c_{j,\ell}} = \frac{\varphi_{j,\ell}/\xi}{c_{j,\ell}}, \tag{36}$$

where ξ is the wavenumber and $\varphi_{j,\ell}$ is the dispersion angular frequency determined by plane wave theory applied to the recursion formula (29). Taking

$$u_{j,\ell}^k = e^{i(\xi_x x_j + \xi_z z_\ell - \varphi_{j,\ell} t_k)}, \tag{37}$$

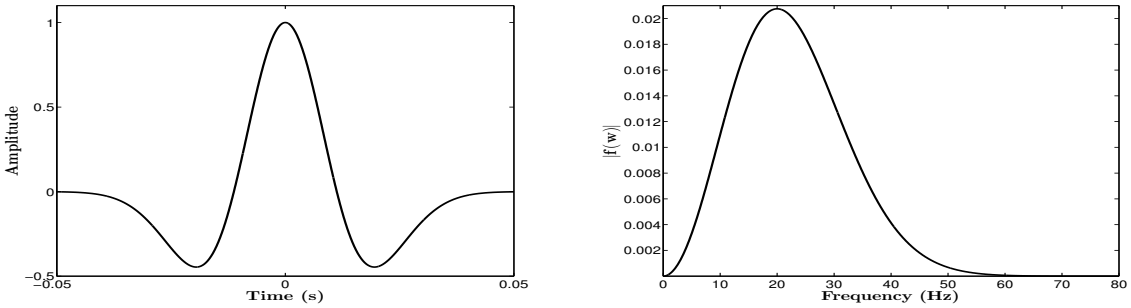

Figure 5: Source wavelet in time (left) and frequency (right) domain.

where $\xi_x = \xi \cos\theta$, $\xi_z = \xi \sin\theta$, θ is the propagation angle, and substituting it into equation (29), we find

$$\varphi_{j,\ell} = \frac{2}{\Delta t} \arcsin \sqrt{r_{j,\ell}^2 \sum_{m=1}^{M} a_{m,j,\ell} \left[\sin^2\left(\frac{m\cos(\theta\gamma)}{2}\right) + \sin^2\left(\frac{m\sin(\theta\gamma)}{2}\right)\right]}, \tag{38}$$

where $\gamma = \xi \Delta x$. Therefore,

$$\psi_{j,\ell} = \frac{2}{r_{j,\ell}\gamma} \arcsin \sqrt{r_{j,\ell}^2 \sum_{m=1}^{M} a_{m,j,\ell} \left[\sin^2\left(\frac{m\cos(\theta\gamma)}{2}\right) + \sin^2\left(\frac{m\sin(\theta\gamma)}{2}\right)\right]}. \tag{39}$$

Observe that $\psi_{j,\ell} \equiv \psi_{j,\ell}(\theta) = \psi_{j,\ell}(\pi/2 \pm \theta)$, and then we can compute $\psi_{j,\ell}$ only for $\theta \in [0, \pi/4]$. In the right of Figure 4 we can observe the dispersion curves $\psi_{j,\ell}$ in the case of $M = 10$, $c = 3$ km/s, $\Delta x = 0.01$ km, $\Delta t = 0.001$ s, for different values of the propagation angle. We can observe that $\theta = \pi/4$ is the value for which $\psi_{j,\ell} \approx 1$, and it is this value that we are going to use in the numerical experiments.

The Choice for Δx, Δz, Δt and M

The choice of parameters $\Delta = \Delta x = \Delta_z$ and Δt is as in the one-dimensional case. For a fixed maximum error $\eta > 0$, we choose $M_{j,\ell}$ as the minimum $M \geq M_{min}$ such that

$$\mu(M, c_{j,\ell}) = \left| \frac{\Delta}{v_j, \ell} - \frac{\Delta}{c_{j,\ell}} \right| = \frac{\Delta x}{c_{j,\ell}} \left| \frac{1}{\psi_{j,\ell}} - 1 \right| < 1. \tag{40}$$

NUMERICAL EXPERIMENTS

In this section we presente the numerical simulations for the one- and two-dimensional cases, for a source term given by $F(\mathbf{x}, t) = \delta(\mathbf{x} - \mathbf{x}_S) g(t)$, where δ is the Dirac's delta function, $\mathbf{x}_S$ is the source position, and g is a Ricker wavelet, with peak frequency of 20 Hz,

$$g(t) = (1 - 2(20\pi t)^2) e^{-(20\pi t)^2}. \tag{41}$$

as illustrated in Figure 5. For the discretization, we have

$$F(x_j, t_k) = \frac{1}{\Delta x} \delta_{j,j_S} s(t_k) \quad \text{or} \quad F(x_j, z_\ell, t_k) = \frac{1}{\Delta^2} \delta_{j,j_S} \delta_{\ell,\ell_S} g(t_k), \tag{42}$$

where j_S and ℓ_S are the indices for the source position and $\delta_{p,q}$ denotes the Kronecker delta. Regarding the boundary conditions, we used a time window $[0, T_{max}]$ and a large box in the space domain to avoid unwanted reflections from the boundary.

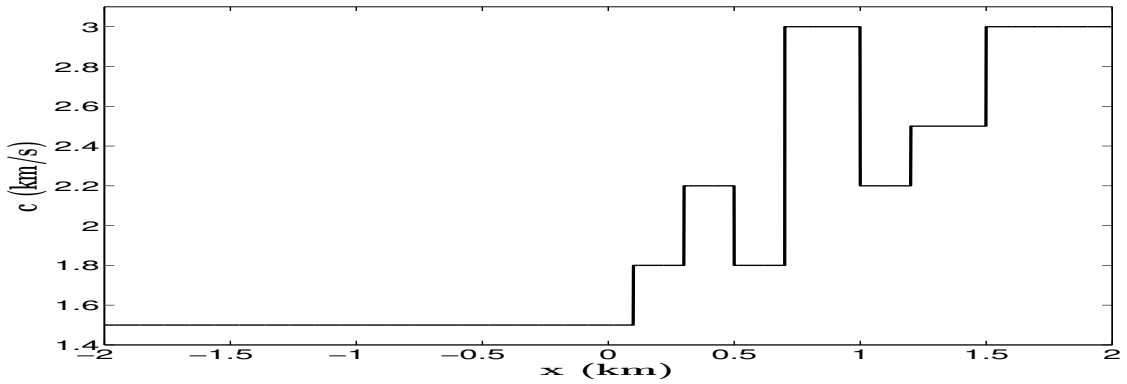

Figure 6: Velocity profile.

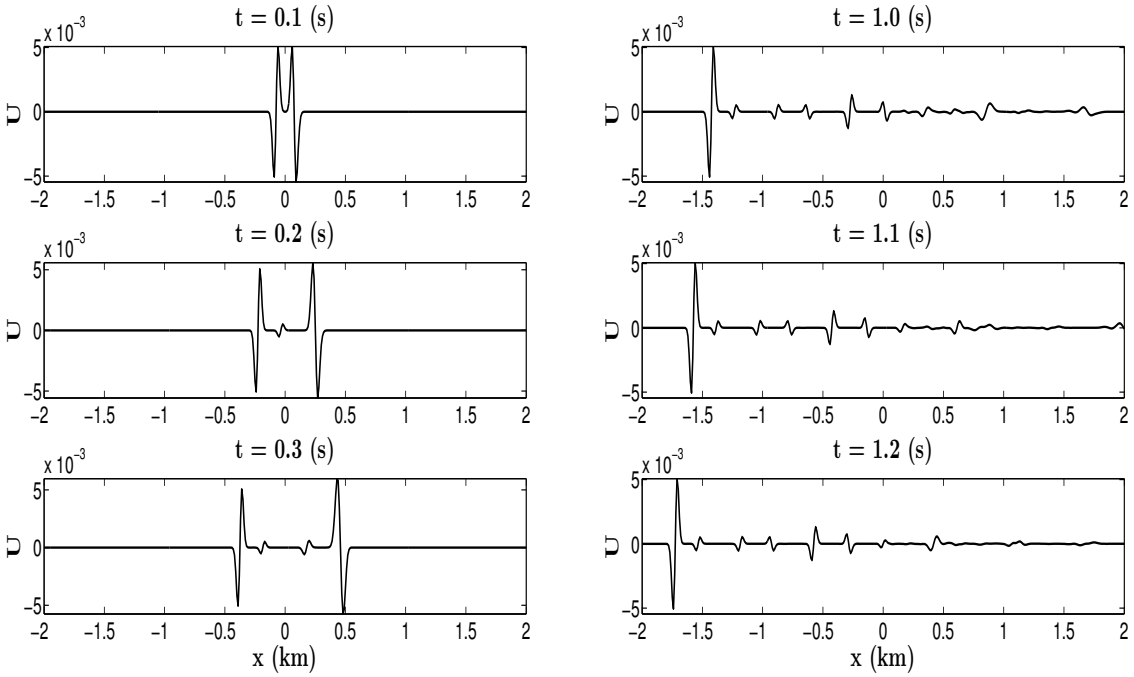

Figure 7: One-dimensional solution using the adaptive scheme.

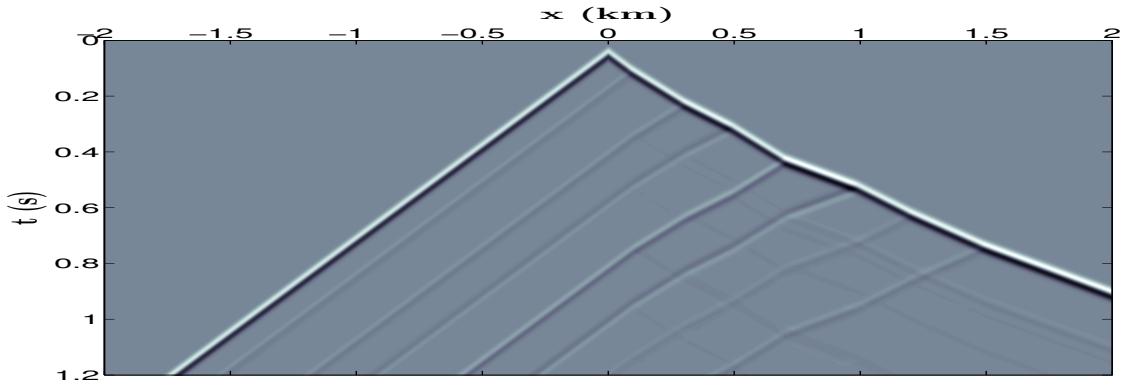

Figure 8: Full seismogram for the one-dimensional case.

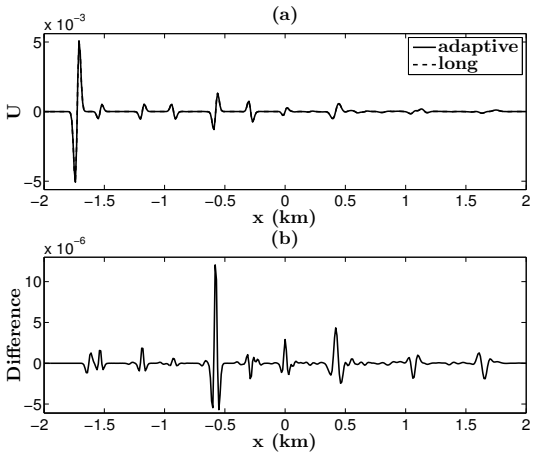

Figure 9: (a) Comparison of the solutions between adaptive FD and conventional FD with a long spatial operator. (b) Difference.

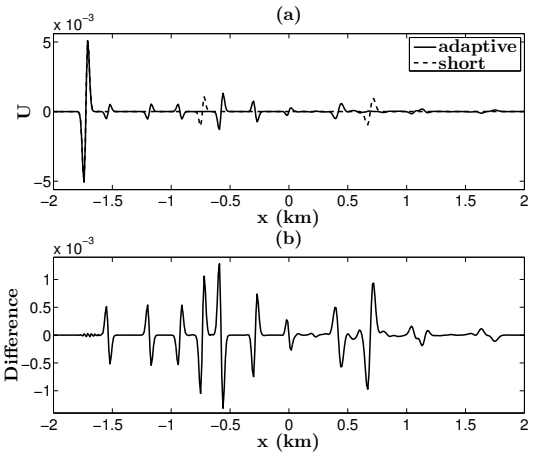

Figure 10: (a) Comparison of the solutions between adaptive FD and conventional FD with a short spatial operator. (b) Difference.

One-Dimensional Modeling

We used the following parameters: $\Delta x = 10$ m, $\Delta t = 1$ ms, $\eta = 10^{-3}$, $x_S = 0$, and the velocity profile depicted in Figure 6. Figure 7 shows the solution of the adaptive FD schemes for some time values, and in Figure 8 we show the full seismogram.

We compare the solutions for different choices of the length operator: (i) M computed in the adaptive way, (ii) M fixed and based on the lowest velocity (long), (iii) M fixed and based on the highest velocity (short), and (iv) $M = M_{min} = 2$ (since depending on the velocity, M may not reach M_{min}).

In Figures 9 and 10 we compare the solutions from the adaptive scheme and the ones computed with a conventional FD scheme with long and short spatial operators. We can observe that there is no significant dispersion, as expected, whereas in Figure 11, which depicts the solution using $M = M_{min}$, the dispersion is significant. Figure 12 shows the value of the length operator chosen by the method (23).

To validate our algorithm, we also compared the solution from the FD schemes with the analytical solution of the wave equation with constant velocity (negative x in the model). The results, for two different times, are shown in Figures 13 and 14. To compare the computational effort of the algorithms, in Figure 15 we show the computational times for the algorithms, for different values of η.

Two-DimensionalModeling

For the two-dimensional modeling we used the following paramenters: $\Delta x = 10$ m, $\Delta t = 0.001$ ms, $\eta = 10^{-4}$, $\mathbf{x}_S = (0, 0)$, and with the velocity model shown in Figure 16. The snapshots for the adptive scheme are show in Figures 17 and 18, and Figure 19 depicts the variation of the length operator M with the velocity.

Figures 20 and 21 show the solutions from the adaptive scheme and the ones computed with a conventional FD scheme with long and short spatial operators. Figure 22 exhibit the computational time for the algorithms only for $\eta = 10^{-4}$.

CONCLUSIONS

We tested the adaptive FD scheme for the acoustic wave equation proposed by Liu and Sen (2011). The advantage of the new approach is that it is possible to have a better accuracy than the conventional method with the same discretization. We presented dispersion and stability analysis, with sopme numerical experiments.

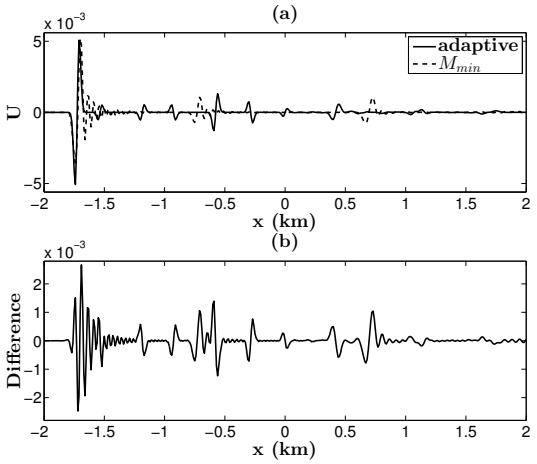

Figure 11: (a) Comparison of the solutions between adaptive FD and conventional FD with $M = M_{min}$. (b) Difference.

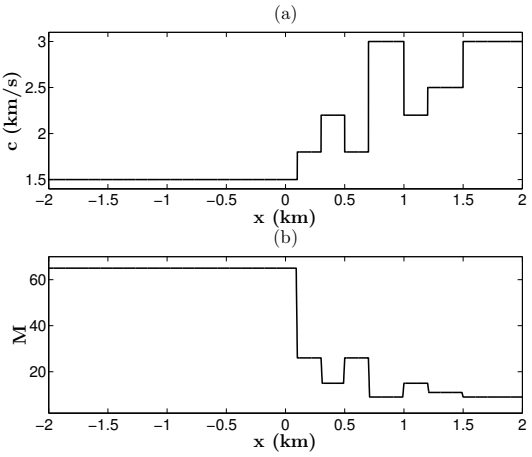

Figure 12: (a) Velocity profile. (b) Variation of the length operator M according to the velocity profile, for $\eta = 10^{-3}$.

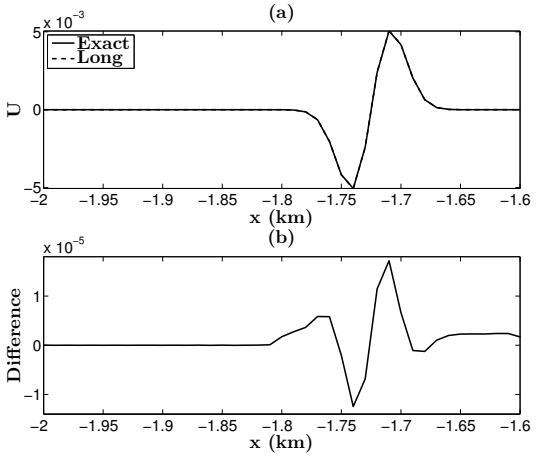

Figure 13: (a) Comparison of the conventional FD (long operator) and exact solution (homogeneous case). (b) Difference.

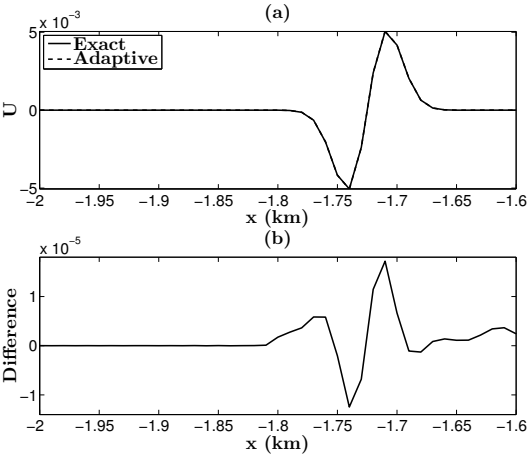

Figure 14: (a) Comparison of the adaptive and exact solution (homogeneous case). (b) Difference.

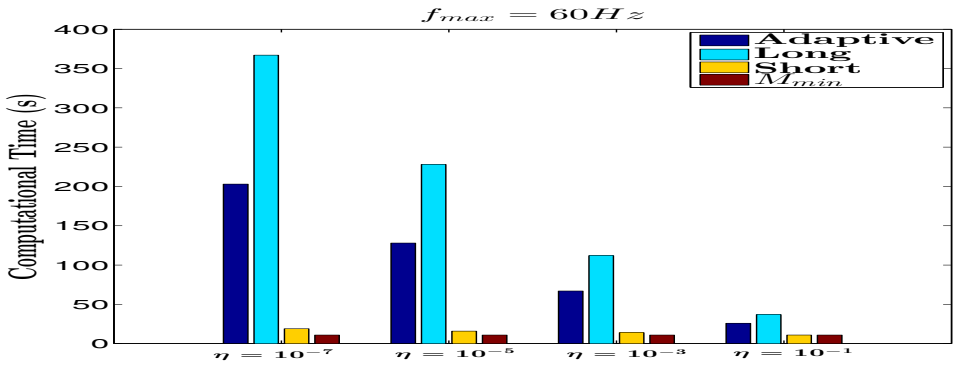

Figure 15: Computational time for different values of η.

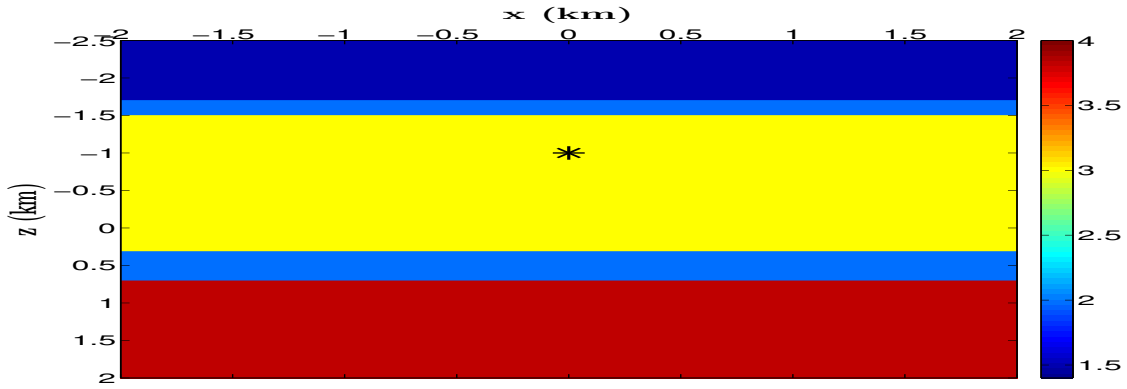

Figure 16: Two-dimensional velocity model, where the $*$ indicates the source position. The colorbar indicates de velocity in km/s.

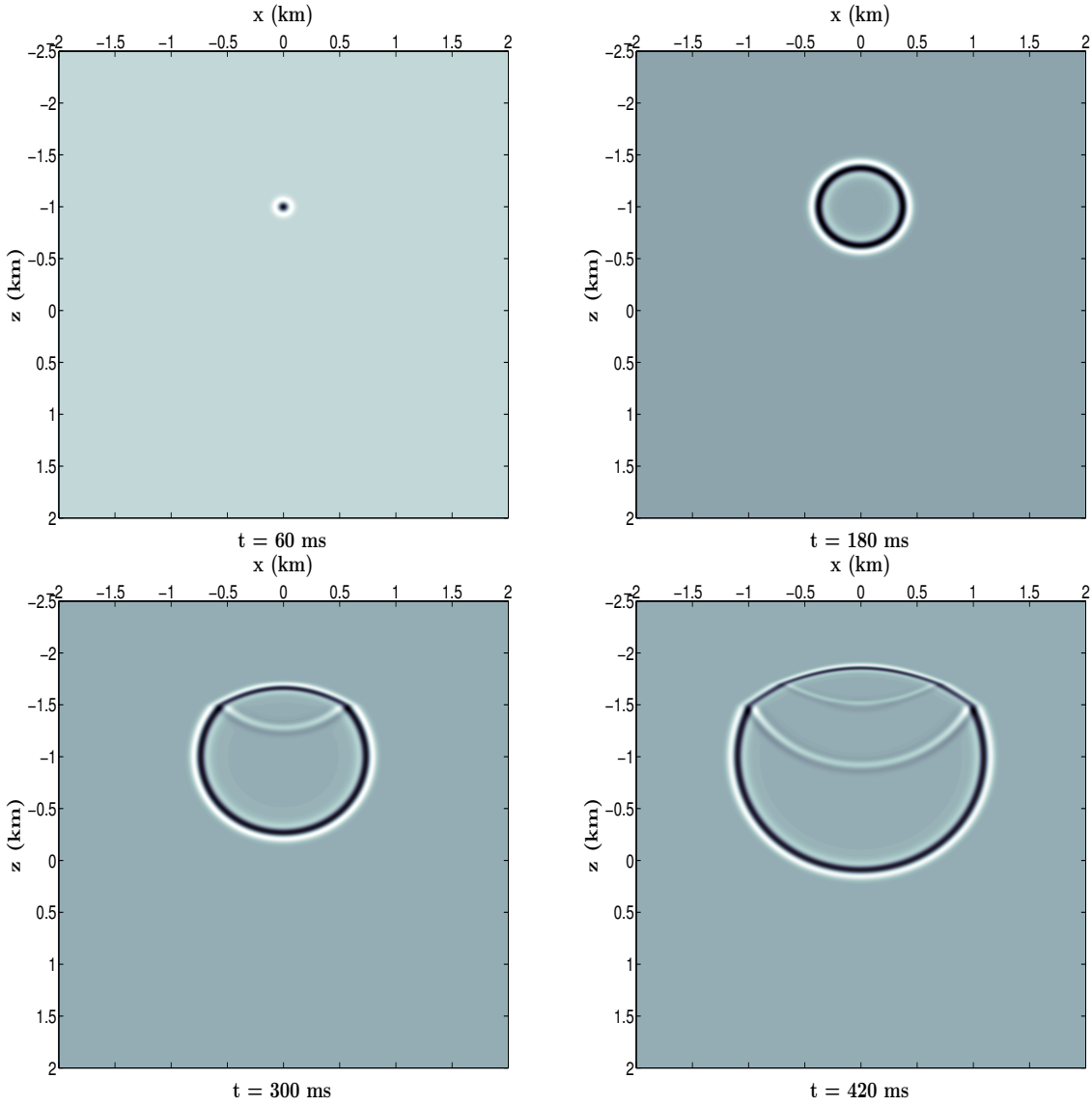

Figure 17: Snapshots for the two-dimensional solution computed with the adaptive FD scheme.

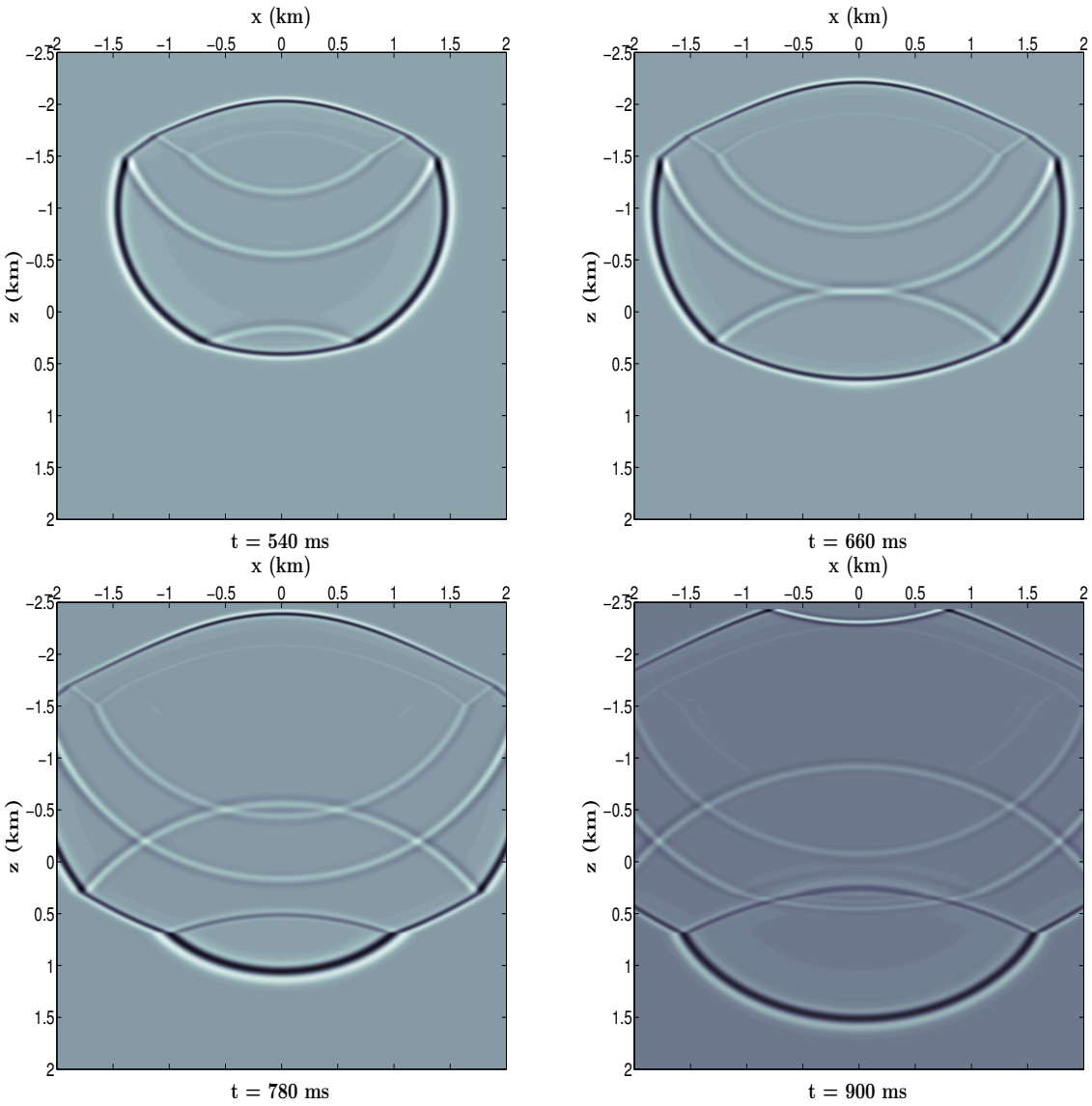

Figure 18: Snapshots for the two-dimensional solution computed with the adaptive FD scheme.

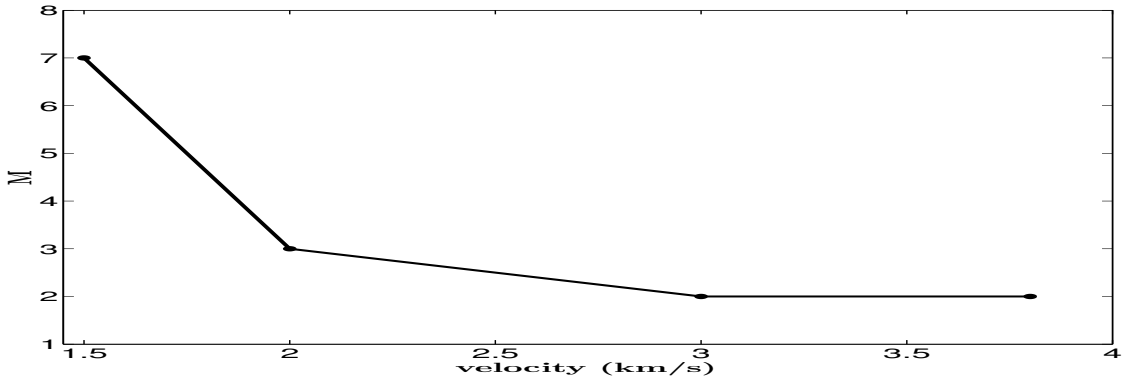

Figure 19: Variation of the length operator M with the velocity, for $\eta = 10^{-4}$.

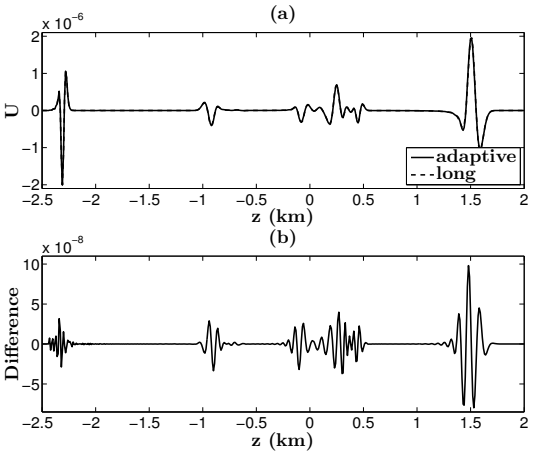

Figure 20: (a) Comparison of the solutions between adaptive FD and conventional FD with a long spatial operator. (b) Difference.

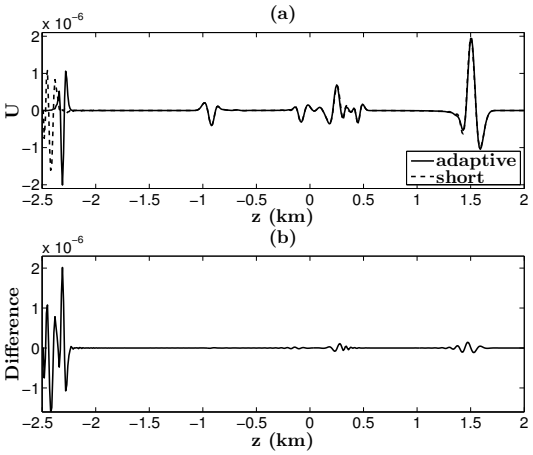

Figure 21: (a) Comparison of the solutions between adaptive FD and conventional FD with a short spatial operator. (b) Difference.

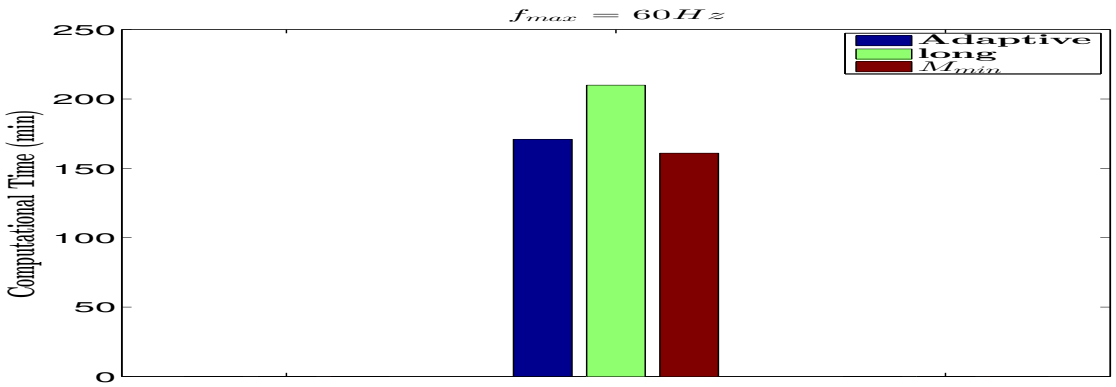

Figure 22: Computational time for $\eta = 10^{-4}$.

ACKNOWLEDGEMENTS

This work was kindly supported by the research agencies CAPES and CNPq, Brazil, and the sponsors of the Wave Inversion Technology (WIT) Consortium, Germany.

REFERENCES

Bartolo, L. D., Dors, C., and Mansur, W. J. (2012). A new family of finite difference schemes to solve the heterogeneuos acoustic wave equation. *Geophysics*, 77:T187–T199.

Dablain, M. A. (1986). The application of high-order differencing to the scalar wave equation. *Geophysics*, 51:54–56.

Finkelstein, B. and Kastner, R. (2007). Finite difference time domain dispersion reduction schemes. *Computational Physics*, 221:422–438.

Kelly, K. R., Ward, R. W., Treitel, S. W., and Alford, R. M. (1976). Synthetic seismogram: a finite difference approach. *Geophysics*, 41:2–27.

Liu, Y. and Sen, M. K. (2009). A new time-space domain high-order finite-difference method for the acoustic wave equation. *Computational Physics*, 228(23):8779–8806.

Liu, Y. and Sen, M. K. (2011). Finite-difference modeling with adaptive variable-length spatial operators. *Geophysics*, 76:T79–T89.

Strikwerda, J. C. (1989). *Finite difference shemes and partial differential equations*. Wadsworth & Brooks/Cole Mathematics Series.

Virieux, J. (1984). Sh wave propagation in heterogeneous media: velocity-stress finite difference method. *Geophysics*, 49:1933–1957.

Virieux, J. (1986). P-sv wave propagation in heterogeneous media: velocity-stress finite difference method. *Geophysics*, 51:889–991.